

A NEW FAINT MILKY WAY SATELLITE DISCOVERED IN THE PAN-STARRS1 3π SURVEY

BENJAMIN P. M. LAEVENS^{1,2}, NICOLAS F. MARTIN^{1,2}, RODRIGO A. IBATA¹, HANS-WALTER RIX², EDOUARD J. BERNARD³, ERIC F. BELL⁴, BRANIMIR SESAR², ANNETTE M. N. FERGUSON³, EDWARD F. SCHLAFLY², COLIN T. SLATER⁴, WILLIAM S. BURGETT⁵, KENNETH C. CHAMBERS⁶, HEATHER FLEWELLING⁶, KLAUS A. HODAPP⁶, NICHOLAS KAISER⁶, ROLF-PETER KUDRITZKI⁶, ROBERT H. LUPTON⁷, EUGENE A. MAGNIER⁶, NIGEL METCALFE⁸, JEFFREY S. MORGAN⁶, PAUL A. PRICE⁷, JOHN L. TONRY⁶, RICHARD J. WAINCOAT⁶, CHRISTOPHER WATERS⁶

Draft version July 23, 2018

ABSTRACT

We present the discovery of a faint Milky Way satellite, Laevens 2/Triangulum II, found in the Panoramic Survey Telescope And Rapid Response System (Pan-STARRS 1) 3π imaging data and confirmed with follow-up wide-field photometry from the Large Binocular Cameras. The stellar system, with an absolute magnitude of $M_V = -1.8 \pm 0.5$, a heliocentric distance of 30_{-2}^{+2} kpc, and a half-mass radius of 34_{-8}^{+9} pc, shows remarkable similarity to faint, nearby, small satellites such as Willman 1, Segue 1, Segue 2, and Boötes II. The discovery of Laevens 2/Triangulum II further populates the region of parameter space for which the boundary between dwarf galaxies and globular clusters becomes tenuous. Follow-up spectroscopy will ultimately determine the nature of this new satellite, whose spatial location hints at a possible connection with the complex Triangulum-Andromeda stellar structures.

Subject headings: Local Group — Milky Way, satellites, streams: individual: Laevens 2/Triangulum II

1. INTRODUCTION

The last couple of decades saw the discovery of numerous satellites in the Milky Way (MW) halo. While the Sloan Digital Sky Survey (SDSS (York et al. 2000)) satellite discoveries have provided us with greater observational constraints in our backyard, especially to understand the faint end of galaxy formation in the preferred cosmological paradigm of Λ CDM (Belokurov 2013), they have also led to debates about the nature of the faintest satellites (Gilmore et al. 2007). It has become apparent that the previously clear distinction between the compact globular clusters (GCs) and the brighter, more extended, and dark-matter dominated dwarf galaxies (DGs), blurs out for faint systems (Willman & Strader 2012). This is exemplified by the discoveries of Willman 1 (Will; Willman et al. 2005) and Segue 1 (Seg1; Belokurov et al. 2007), followed up by those of Boötes II (BooII; Walsh et al. 2007), and Segue 2 (Seg2; Belokurov et al. 2009), all nearby satellites within 25–45 kpc, and just slightly larger than extended outer halo GCs. At the same time, these systems are fainter than most GCs and all the other DGs. Theoretical expec-

tations show that these objects could well be the faintest DGs and that tens or hundreds of DGs with these properties could populate the Milky Way halo (Tollerud et al. 2008; Hargis et al. 2014). As of yet, just two objects have been found in the PS1 survey (Laevens et al. 2014), reinforcing the tension between theory and observations (Klypin et al. 1999). Only the closest DGs would be detected with current photometric surveys (Koposov et al. 2007; Walsh et al. 2009). Spectroscopic studies do show that the faint systems found so far are dynamically hotter than their mere stellar content would imply, hinting that they are indeed DGs (Martin et al. 2007; Willman et al. 2011; Simon et al. 2011; Kirby et al. 2013). However, the low velocity dispersion of these satellites ($< 4 \text{ km s}^{-1}$), combined with the possibly large impact of binaries (McConnachie & Côté 2010), the complexity of disentangling member stars from foreground contaminants, and the overall dimness of their member stars renders any definite conclusion difficult.

Here, we present the discovery of another faint MW satellite, Laevens 2/Triangulum II⁹, with very similar photometric properties to Will1, Seg1, BooII, and Seg2. The new system was found in our ongoing effort to mine the Pan-STARRS 1 (PS1) 3π survey for localized stellar overdensities. This letter is structured as follows: in section 2, we describe the PS1 survey along with the detection method that led to the discovery. We continue by discussing follow-up imaging obtained with the Large Binocular Cameras in section 3. We discuss the nature of the satellite and its implication in section 4. In the final section, we summarize and conclude our results.

In this paper, magnitudes are dereddened using the Schlegel et al. (1998) maps, adopting the extinction co-

⁹ In the absence of spectroscopic confirmation, we wish to remain agnostic about the nature of this object and therefore propose a double name. For future reference in this paper, we abbreviate to Lae 2/Tri II.

benjamin.laevens@astro.unistra.fr

¹ Observatoire astronomique de Strasbourg, Université de Strasbourg, CNRS, UMR 7550, 11 rue de l'Université, F-67000 Strasbourg, France

² Max-Planck-Institut für Astronomie, Königstuhl 17, D-69117 Heidelberg, Germany

³ Institute for Astronomy, University of Edinburgh, Royal Observatory, Blackford Hill, Edinburgh EH9 3HJ, UK

⁴ Department of Astronomy, University of Michigan, 500 Church St., Ann Arbor, MI 48109, USA

⁵ GMTO Corporation, 251 S. Lake Ave, Suite 300, Pasadena, CA 91101, USA

⁶ Institute for Astronomy, University of Hawaii at Manoa, Honolulu, HI 96822, USA

⁷ Department of Astrophysical Sciences, Princeton University, Princeton, NJ 08544, USA

⁸ Department of Physics, Durham University, South Road, Durham DH1 3LE, UK

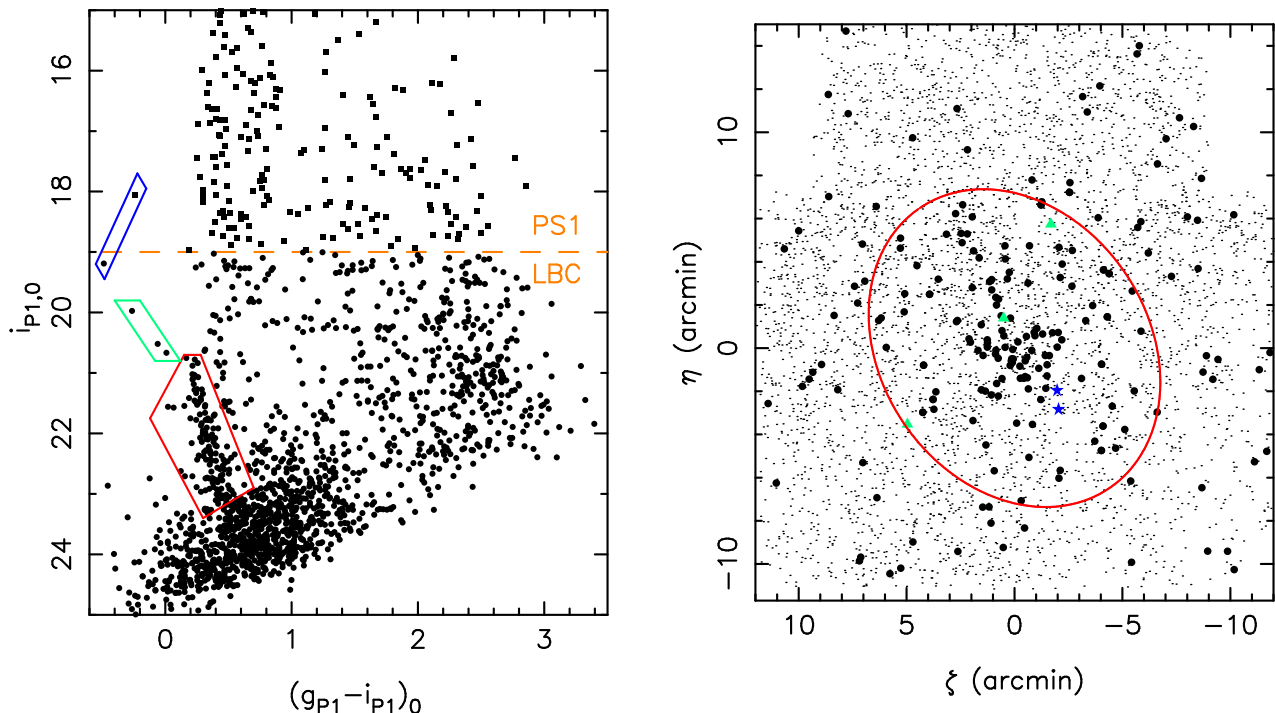


Figure 1. : *Left*: The combined PS1-LBC CMD of all sources within the central $2r_h$ region of Lae 2/Tri II. The single epoch PS1 photometry was used at the bright end ($i_{P1,0} < 19$, squares), with LBC photometry supplementing the faint end $i_{P1,0} > 19$ (large dots). The orange dashed line indicates the separation between the LBC and PS1 data. The red box highlights the clear main sequence of the stellar system, the blue box indicates two possible HB stars and the green box identifies likely blue stragglers. *Right*: Spatial distribution of all sources corresponding to the CMD on the left. Large dots correspond to the stars falling within the red CMD box in the left panel and show a clear overdensity. The two blue stars indicate the possible HB stars whereas the red ellipse corresponds to the region within the favored two half-mass radius of the system, as inferred below.

efficients of Schlafly & Finkbeiner (2011). A heliocentric distance of 8 kpc to the Galactic center is assumed.

2. THE 3π PS1 SURVEY AND DISCOVERY

With a spatial extent encompassing three quarters of the sky ($\delta > -30^\circ$), PS1 (K. Chambers et al., in preparation) gives us an unprecedented panoramic view of the MW and its surroundings. Over the course of 3.5 years, the 1.8m telescope, equipped with its 1.4-gigapixel camera covering a 3.3-degree field of view, has collected up to four exposures per year in each of 5 bands ($g_{P1}r_{P1}i_{P1}z_{P1}y_{P1}$; Tonry et al. 2012). A photometric catalogue is automatically generated with the Image Processing Pipeline (Magnier 2006, 2007; Magnier et al. 2008), once the individual frames have been downloaded from the summit. The preliminary stacked photometry used in this paper has a g_{P1} depth (23.0) that is comparable to SDSS g -band depth and r_{P1}/i_{P1} observations that reach $\sim 0.5/\sim 1.0$ magnitude fainter: 22.8, 22.5 for r and i respectively (Metcalf et al. 2013).

Inspired by past searches for small stellar overdensities in MW and M31 surveys, we apply a convolution technique (Laevens et al., in preparation), successfully used to find new GCs and DGs in the SDSS (Koposov et al. 2007; Walsh et al. 2009). In a nutshell, we build a mask in $(r - i, i)$ color-magnitude space to isolate potential metal-poor, old, and blue member stars that could belong to a MW satellite at a chosen distance. This mask is applied to star-like sources in the stacked PS1 photometric catalog. We then convolve the distribution of isolated sources with two Gaussian spatial filters: a positive

Gaussian tailored to the size of the overdensities we are searching for ($2'$, $4'$, or $8'$) and a negative Gaussian with a much larger kernel ($14'$, $28'$, or $56'$), to account for the slowly-varying contamination of sources that fall within the color-magnitude mask. By convolving the data with the sum of these two (positive and negative) filters and accounting for the survey's spatial incompleteness on the arcminute scale, we obtain maps tracking stellar over- and under-densities in PS1. We convert these density maps into maps of statistical significance by comparison with the neighboring regions after cycling through distances and filter sizes. This procedure already led to the discovery of Laevens 1¹⁰ (Laevens et al. 2014) also discovered concomitantly as Crater within the ATLAS survey by Belokurov et al. (2014). The new satellite, Lae 2/Tri II, is located $\sim 20^\circ$ East of M31 and appears as a 5.2σ detection, only slightly higher than our significance criteria of 5σ ¹¹ tailored to weed out spurious detections.

3. FOLLOW-UP

To confirm the nature and the properties of Lae 2/Tri II, follow-up imaging was obtained with the Large Binocular Camera (LBC) on the Large Binocular Telescope (LBT), located on Mount Graham, USA during the night of October 17–18 2014. With its $23' \times 25'$

¹⁰ Following the naming convention established in Bianchini et al. (2015)

¹¹ These also include a check that potential detections do not also correspond to a significant overdensity of background galaxies (Koposov et al. 2007).

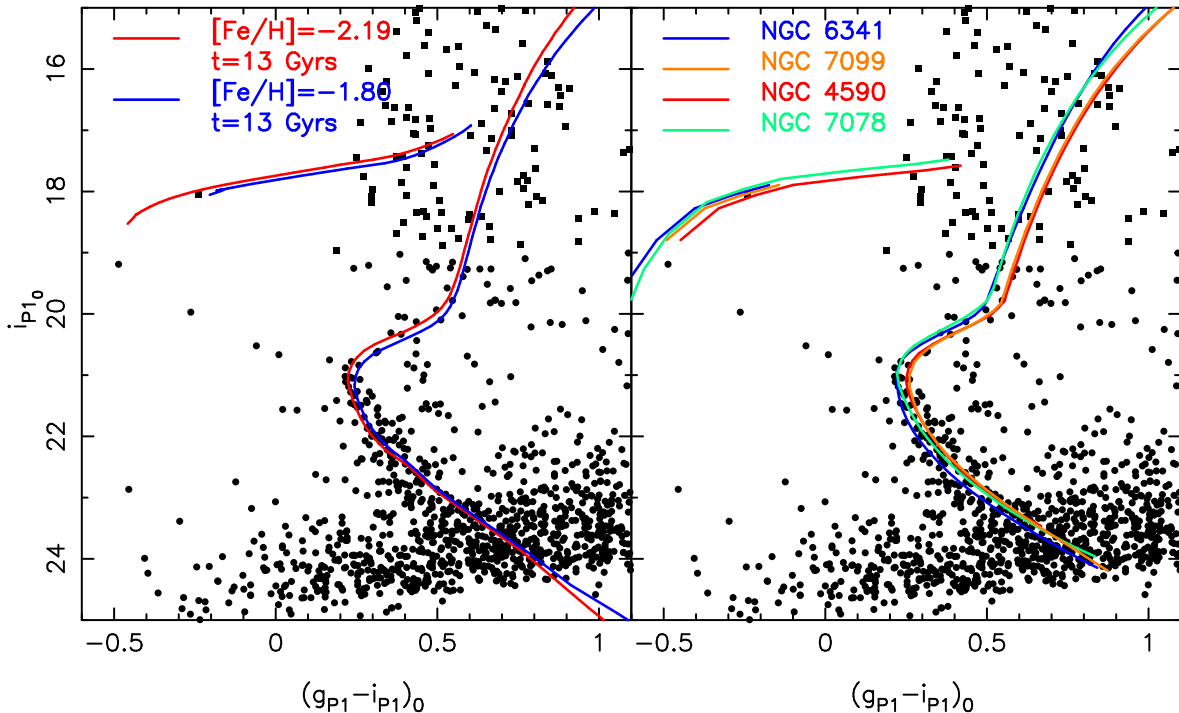


Figure 2. *Left:* The CMD of Lae 2/Tri II within $2r_h$, with best-fit isochrones overlotted. Both isochrones have an age of 13 Gyr and are shifted to a distance modulus of 17.3. The red/blue isochrones have metallicities $[\text{Fe}/\text{H}] = -2.19$ and $[\text{Fe}/\text{H}] = -1.80$, respectively. *Right:* The same CMD of Lae 2/Tri II with four metal-poor fiducial isochrones from GCs observed in PS1 (Bernard et al. 2014), dereddened assuming the reddening values of (Harris 2010) and shifted to match the observed features. The green fiducial (NGC 7078; $[\text{Fe}/\text{H}] = -2.37$), shifted to a distance-modulus of 17.5 best represents the features of the new stellar system, with the other fiducials i.e. red: NGC 4590 ($[\text{Fe}/\text{H}] = -2.23$), blue: NGC 6341 ($[\text{Fe}/\text{H}] = -2.31$), orange: NGC 7099 ($[\text{Fe}/\text{H}] = -2.27$) appearing too red or too blue to accurately reproduce the MS and MSTO. NGC 4590 is shifted to a distance-modulus of 17.5, whereas NGC 6341 and 7099 are at 17.3.

field of view and equipped with 4 CCDs, the LBC are ideal to follow-up MW satellites that usually span a few arcminutes on the sky. Imaging was conducted in the g and i bands, making use of the time-saving dual (binocular) mode using the red and blue eye simultaneously. Six dithered 200s sub-exposures were acquired in each band, with a seeing of $1''$. The field was centered on the location of Lae 2/Tri II.

The images were processed and the photometry performed using a version of the CASU pipeline (Irwin & Lewis 2001) updated to work on LBC data. The instrumental magnitudes were calibrated onto the PS1 system (g_{P1} and i_{P1}), by comparison with the PS1 single epoch data (Schlafly et al. 2012) to derive the relevant color equations. The final LBC photometry reaches more than 2 magnitudes deeper than the stacked PS1 data. The left-hand panel of Figure 1 shows the combined PS1/LBC color-magnitude diagram (CMD) of all stars within 2 half-light radii ($\pm 2r_h$), for which all sources brighter than $i_{P1,0} = 19.0$ are taken from the PS1 single epoch photometry so as to extend the CMD beyond the saturation limit of the LBC photometry. The main sequence (MS) of an old and metal-poor stellar system is readily visible, with a clear turn off at $i_{P1,0} \sim 20.8$. Given the low density of the MS, the red giant branch (RGB) of the stellar system is very likely sparsely populated and hidden within the foreground contamination of bright stars. However, two blue stars are consistent with being blue horizontal branch (HB) stars and are highlighted in the CMD. The other panel of Figure 1 presents the spatial distribution of sources in the four

chips, with a red ellipse indicating the satellite’s two half-light radii extent (as determined by the structural parameter analysis, see section 4). Stars with colors and magnitudes consistent with the MS are shown as large dots and reveal a clear spatial overdensity. Likely blue straggler stars are identified and given by the green triangles. The two blue stars correspond to the potential HB stars; their location close to the center of the stellar overdensity supports them being member HB stars.

4. PROPERTIES OF THE STELLAR SYSTEM

Since the RGB and HB are so sparsely populated, an investigation into the presence of member RR Lyrae stars in the multi-epoch PS1 data unsurprisingly led to no candidate from which to derive a distance estimate. However, due to the well defined MS and MS turnoff (MSTO) at $i_{P1,0} \sim 20.8$, a reliable distance estimate can nevertheless be determined through a comparison with isochrones and fiducials by eye (Figure 2). We assess the stellar system’s metallicity, age, and distance modulus by first cycling through PARSEC isochrones (Bressan et al. 2012) for a metallicity range $-2.2 < [\text{Fe}/\text{H}] < -1.3$ ($Z = 0.0001$ to 0.0007 , assuming $Z_{\odot} = 0.152$) and an age between 9 and 13 Gyr. We investigate the effects that various metallicities and ages have on the distance determination, by cycling through distance-modulus steps of 0.1 between 16.9 and 17.5. The isochrone which best represents the CMD features is a metal-poor, old isochrone ($[\text{Fe}/\text{H}] = -2.19$ and age of 13 Gyrs), for a distance modulus of 17.3. We further strengthen these conclusions by comparing the CMD of Lae 2/Tri II with the fiducials

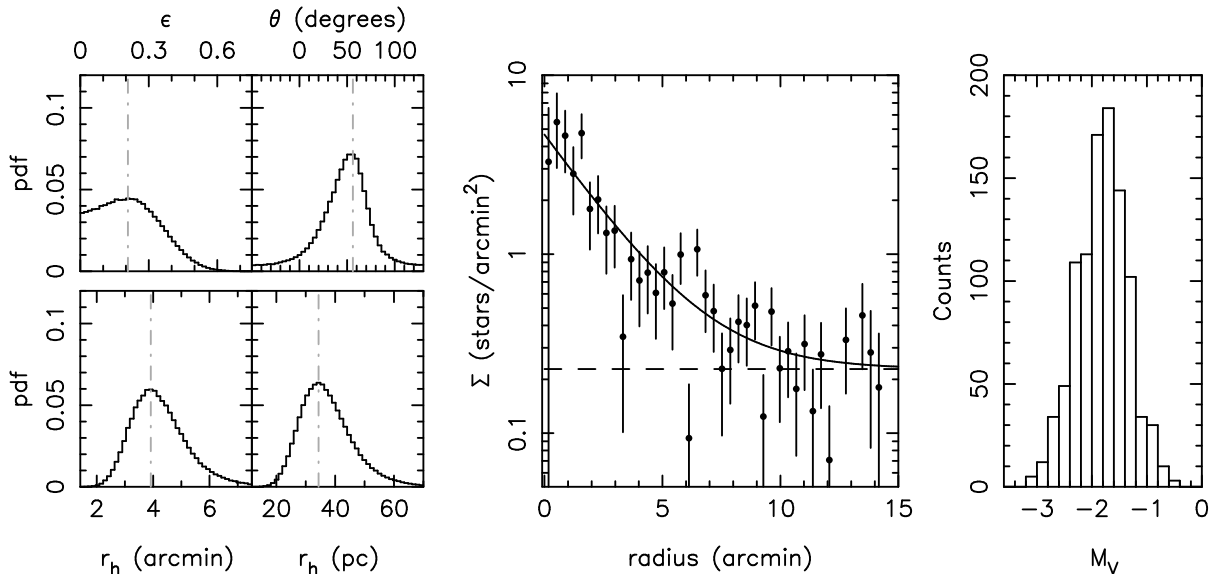


Figure 3. *Left:* Probability distribution functions for the ellipticity (ϵ), the position angle (θ), the angular and the physical half-mass radii (r_h) of Lae 2/Tri II (from top left to bottom right). *Middle:* Comparison between the favored radial distribution profile (full line) and the data, binned according to the preferred structural parameters (dots). The error bars assume Poissonian uncertainties and the dashed line represents the field density. *Right:* Probability distribution function of the absolute magnitude of Lae 2/Tri II in the V band ($M_V = -1.8 \pm 0.5$).

from 13 GCs and 3 Open Clusters of varying metallicity, derived directly from the PS1 data (Bernard et al. 2014). The 4 most metal-poor GCs of the sample provide a good fit to the MS and MSTO of Lae 2/Tri II provided they are shifted to distance moduli in the 17.3-17.5 range.

Combining these two analyses by averaging the six best-fits fiducials and isochrones, we therefore conclude that Lae 2/Tri II is old and metal-poor, and is located at a distance modulus of $17.4^{+0.1}_{-0.1}$, which translates to a heliocentric distance of 30^{+2}_{-2} kpc, or 36^{+2}_{-2} kpc from the Galactic center. In both cases (isochrone and fiducial), the HB of the favored track also overlaps almost exactly with the two potential HB stars. Please note that the uncertainty in the distance measurement is propagated through for the derivation of the structural parameters, further detailed in the next few paragraphs. We also draw to the reader’s attention that a more involved analysis of ‘CMD-fitting’ would likely enhance the quality of the distance measurement; however, the limitation of the field of view prevent us from obtaining a large enough sample of background stars to perform such an analysis.

We derive the structural parameters of Lae 2/Tri II by using a modified version of the technique described in Martin et al. (2008), updated in Martin et al. (2015, submitted). The updated technique allows for a Markov Chain Monte Carlo (MCMC) approach, based on the likelihood of a family of exponential radial density profiles (allowing for flattening and a constant contamination over the field) to reproduce the distribution of the system’s MS stars. The parameters of the model are: the centroid of the system, its ellipticity¹², its position angle (defined as the angle of the major axis from North to East), its half-mass radius¹³, r_h , and the number of stars,

¹² The ellipticity is here defined as $1 - b/a$ with a and b the major and minor axis scale lengths, respectively.

¹³ Note that, assuming no mass segregation in the system, the

Table 1
Properties of Lae 2/Tri II

| | |
|------------------------------|----------------------------|
| α (J2000) | 02:13:17.4 |
| δ (J2000) | +36:10:42.4 |
| ℓ | 141.4° |
| b | -23.4° |
| Distance Modulus | $\sim 17.4^{+0.1}_{-0.1}$ |
| Heliocentric Distance | 30^{+2}_{-2} kpc |
| Galactocentric Distance | 36^{+2}_{-2} kpc |
| M_V | -1.8 ± 0.5 |
| [Fe/H] | ~ -2.2 |
| Age | ~ 13 Gyr |
| $E(B - V)^a$ | 0.081 |
| Ellipticity | $0.21^{+0.17}_{-0.21}$ |
| Position angle (from N to E) | 56^{+16}_{-24} ° |
| r_h | $3.9^{+1.1}_{-0.9}$ arcmin |
| r_h | 34^{+9}_{-8} pc |

^a from Schlegel et al. (1998)

N^* , within the chosen CMD selection box. Although it is located in the Triangulum constellation, Lae 2/Tri II is so far from both M31 (~ 20 degrees) and M33 (~ 10 degrees) that any contamination by M31 or M33 stellar populations is vanishingly small and does not impact our results. The resulting probability distribution functions are presented in the left-most panels of Figure 3 for the most important parameters and summarized in Table 1. Figure 3 also shows a favorable comparison of the preferred exponential profile with the data binned following the preferred structural parameters.

It should however be noted that the properties of Lae 2/Tri II as observed by the LBC could be slightly biased by the low contrast of the stellar overdensity. Indeed, Muñoz et al. (2012) show that satellite properties

half-mass radius is equivalent to the half-light radius.

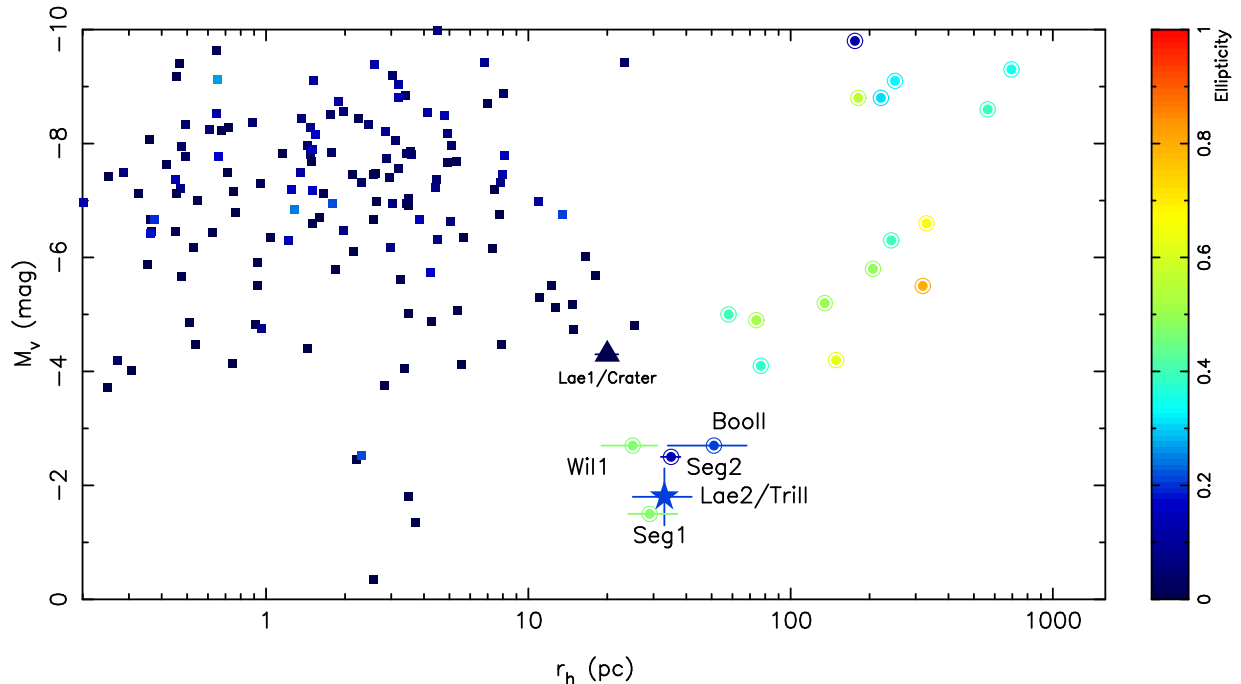


Figure 4. The distribution of MW satellites in size–magnitude space. GCs are shown as squares, DGs are shown as circles and Lae 2/Tri II is represented by the large star symbol. The color scale indicates the ellipticity of the various satellites. Lae 2/Tri II’s ellipticity and half-mass radius show very similar values to those of the four satellites: Seg1, Seg2, BoöII and Will1. Finally, we also indicate the recently discovered MW satellite, Laevens 1/Crater given by the large triangle. The data for the GCs were taken from Harris (2010) and the DGs from McConnachie (2012).

are most accurately measured when the central density of stars relative to that of the background is larger than 20, which is not the case here. Deeper data would be necessary to strengthen our size measurement.

To determine the absolute magnitude of the stellar system, we follow the same procedure we used for Laevens 1/Crater (Laevens et al. 2014) as was initially described in Martin et al. (2008). After drawing a value of N^* from the structural parameter chain, we sample the CMD of the best-fitting Bressan et al. (2012) isochrone (see Figure 2), with its associated luminosity function and photometric uncertainties, until it contains N^* stars in the CMD selection box used for the structural parameter analysis. Adding up the flux of all the stars drawn in this artificial CMD yields the absolute g_{P1} - and i_{P1} -band magnitudes of Lae 2/Tri II ($M_g = -1.7 \pm 0.5$ and $M_i = -2.1 \pm 0.5$), which converts to $M_V = -1.8 \pm 0.5$. This technique has the benefit of accounting for the effect of sampling such a small population of stars may have on the determination of the system’s magnitude (i.e. CMD ‘shot-noise’; Martin et al. 2008).

5. DISCUSSION AND CONCLUSION

We have presented the discovery of a new MW satellite, Lae 2/Tri II, discovered within the PS1 3π data and confirmed from deep and wide LBC follow-up. Located at a heliocentric distance of 30^{+2}_{-2} kpc, this system is very faint ($M_V = -1.8 \pm 0.5$), old (~ 13 Gyrs), metal-poor ($[\text{Fe}/\text{H}] \sim -2.2$), small (34^{+9}_{-8} pc), and mildly elliptical ($0.21^{+0.17}_{-0.21}$). Figure 4 places Lae 2/Tri II in relation to other MW GCs and DGs. This new system’s magnitude and half-mass radius are very similar to the properties of the faint satellites Seg1, Seg2, Will1, and

BoöII, which were all recently discovered in the SDSS. Ultimately, high quality spectroscopic follow-up and an assessment of its dynamics are necessary to confirm the nature of this new satellite. However, its similarity in distance, size, absolute magnitude, age, and metallicity to those of Will1, Seg1, BoöII, and Seg2, that all have larger velocity dispersion than implied by their tiny stellar mass (Martin et al. 2007; Simon et al. 2011; Willman et al. 2011; Kirby et al. 2013) hints that Lae 2/Tri II could well be another one of these systems that appear to populate the faint end of the galaxy realm.

It is also worth noting that the location of Lae 2/Tri II, $(\ell, b) = (141.4^\circ, -23.4^\circ)$, $\sim 20^\circ$ East of M31, places it within the Triangulum-Andromeda stellar structure(s) (TriAnd; Majewski et al. 2004; Rocha-Pinto et al. 2004; Sheffield et al. 2014). Although this MW halo stellar overdensity is very complex, with evidence for multiple substructures (Bonaca et al. 2012; Martin et al. 2013; Martin et al. 2014), it spans a large enough distance range to encompass Lae 2/Tri II ($\sim 15 - 35$ kpc). A recent spectroscopic study of stars within TriAnd by Deason et al. (2014) confirmed that, as initially proposed by Belokurov et al. (2009), Seg2 is also likely embedded within it and follows a systematic trend of these faint satellites being part of MW halo stellar streams. Seg1 has been proposed to be tied to the Orphan Stream (Newberg et al. 2010), though differences in abundance patterns between both have also been observed (Vargas et al. 2013; Casey et al. 2014). Similarly BoöII’s distance and radial velocity are compatible with it being part of the Sagittarius stream (Koch et al. 2009), whereas high resolution abundance measurements for BoöII stars question this association (Koch & Rich

2014). It remains possible, however, that the small stellar systems were satellites of the larger, now disrupted progenitor of these stream, thereby alleviating the need for them to share similar abundances. In this context, it is particularly interesting that Lae 2/Tri II is situated on the linear extrapolation of the Pan-Andromeda Archaeological Survey (PAndAS) MW stream (Martin et al. 2014), 10° beyond the PAndAS footprint where this dwarf galaxy remnant was discovered. The stream and satellite are not aligned; however, the uncertainties on the position angle and ellipticity are not conclusive in ruling this out. Here as well, spectroscopy is necessary to derive the systemic velocity of Lae 2/Tri II and confirm it is compatible with the global motion of Triangulum-Andromeda and, in particular, with the velocity of the PAndAS MW stream. Follow-up will help reinforce or disprove such a hypothesis.

Although PS1 is only slightly deeper than the SDSS, the extra coverage provided by its 3π footprint leaves hope for more discoveries of faint objects like Lae 2/Tri II. Building up the statistics of these systems through more discoveries in current (PS1) and (DES; The Dark Energy Survey Collaboration 2005) or future surveys (LSST; Tyson 2002) is essential if we are to understand the true nature of these incredibly faint stellar systems that can only be found in the MW surroundings.

B.P.M.L. acknowledges funding through a 2012 Strasbourg IDEX (Initiative d'Excellence) grant, awarded by the French ministry of education. N.F.M. and B.P.M.L. gratefully acknowledges the CNRS for support through PICS project PICS06183. H.-W.R. and E.F.T. acknowledge support by the DFG through the SFB 881 (A3). E.F.B. and C.T.S. acknowledge support from NSF grant AST 1008342. We thank the LBT and the observers for the splendid job that enabled the confirmation of this object.

The Pan-STARRS1 Surveys have been made possible through contributions of the Institute for Astronomy, the University of Hawaii, the Pan-STARRS Project Office, the Max-Planck Society and its participating institutes, the Max Planck Institute for Astronomy, Heidelberg and the Max Planck Institute for Extraterrestrial Physics, Garching, the Johns Hopkins University, Durham University, the University of Edinburgh, Queen's University Belfast, the Harvard-Smithsonian Center for Astrophysics, the Las Cumbres Observatory Global Telescope Network Incorporated, the National Central University of Taiwan, the Space Telescope Science Institute, the National Aeronautics and Space Administration under Grant No. NNX08AR22G issued through the Planetary Science Division of the NASA Science Mission Directorate, the National Science Foundation under Grant No. AST-1238877, the University of Maryland, and Eotvos Lorand University (ELTE).

REFERENCES

- Belokurov, V. 2013, *New Astronomy Review*, 57, 100
 Belokurov, V., Irwin, M. J., Koposov, S. E., Evans, N. W., Gonzalez-Solares, E., Metcalfe, N., & Shanks, T. 2014, *ArXiv e-prints*
 Belokurov, V., et al. 2009, *MNRAS*, 397, 1748
 —. 2007, *ApJ*, 654, 897
 Bernard, E. J., et al. 2014, *MNRAS*, 442, 2999
 Bianchini, P., Renaud, F., Gieles, M., & Varri, A. L. 2015, *MNRAS*, feb, L40
 Bonaca, A., Geha, M., & Kallivayalil, N. 2012, *ApJ*, 760, L6
 Bressan, A., Marigo, P., Girardi, L., Salasnich, B., Dal Cero, C., Rubele, S., & Nanni, A. 2012, *MNRAS*, 427, 127
 Casey, A. R., Keller, S. C., Da Costa, G., Frebel, A., & Maunder, E. 2014, *ApJ*, 784, 19
 Deason, A. J., et al. 2014, *MNRAS*, 444, 3975
 Gilmore, G., Wilkinson, M. I., Wyse, R. F. G., Kley, J. T., Koch, A., Evans, N. W., & Grebel, E. K. 2007, *ApJ*, 663, 948
 Hargis, J. R., Willman, B., & Peter, A. H. G. 2014, *ApJ*, 795, L13
 Harris, W. E. 2010, *arXiv:1012.3224*
 Irwin, M., & Lewis, J. 2001, *New Astronomy Review*, 45, 105
 Kirby, E. N., Boylan-Kolchin, M., Cohen, J. G., Geha, M., Bullock, J. S., & Kaplinghat, M. 2013, *ApJ*, 770, 16
 Klypin, A., Kravtsov, A. V., Valenzuela, O., & Prada, F. 1999, *ApJ*, 522, 82
 Koch, A., & Rich, R. M. 2014, *ApJ*, 794, 89
 Koch, A., et al. 2009, *ApJ*, 690, 453
 Koposov, S., et al. 2007, *ApJ*, 669, 337
 Laevens, B. P. M., et al. 2014, *ApJ*, 786, L3
 Magnier, E. 2006, in *The Advanced Maui Optical and Space Surveillance Technologies Conference*
 Magnier, E. 2007, in *Astronomical Society of the Pacific Conference Series*, Vol. 364, *The Future of Photometric, Spectrophotometric and Polarimetric Standardization*, ed. C. Sterken, 153
 Magnier, E. A., Liu, M., Monet, D. G., & Chambers, K. C. 2008, in *IAU Symposium*, Vol. 248, *IAU Symposium*, ed. W. J. Jin, I. Platais, & M. A. C. Perryman, 553–559
 Majewski, S. R., Ostheimer, J. C., Rocha-Pinto, H. J., Patterson, R. J., Guhathakurta, P., & Reitzel, D. 2004, *ApJ*, 615, 738
 Martin, C., Carlin, J. L., Newberg, H. J., & Grillmair, C. 2013, *ApJ*, 765, L39
 Martin, N. F., de Jong, J. T. A., & Rix, H.-W. 2008, *ApJ*, 684, 1075
 Martin, N. F., Ibata, R. A., Chapman, S. C., Irwin, M., & Lewis, G. F. 2007, *MNRAS*, 380, 281
 Martin, N. F., et al. 2014, *ApJ*, 787, 19
 McConnachie, A. W. 2012, *AJ*, 144, 4
 McConnachie, A. W., & Côté, P. 2010, *ApJ*, 722, L209
 Metcalfe, N., et al. 2013, *MNRAS*
 Muñoz, R. R., Padmanabhan, N., & Geha, M. 2012, *ApJ*, 745, 127
 Newberg, H. J., Willett, B. A., Yanny, B., & Xu, Y. 2010, *ApJ*, 711, 32
 Rocha-Pinto, H. J., Majewski, S. R., Skrutskie, M. F., Crane, J. D., & Patterson, R. J. 2004, *ApJ*, 615, 732
 Schlafly, E. F., & Finkbeiner, D. P. 2011, *ApJ*, 737, 103
 Schlafly, E. F., et al. 2012, *ApJ*, 756, 158
 Schlegel, D. J., Finkbeiner, D. P., & Davis, M. 1998, *ApJ*, 500, 525
 Sheffield, A. A., Johnston, K. V., Majewski, S. R., Damke, G., Richardson, W., Beaton, R., & Rocha-Pinto, H. J. 2014, *ApJ*, 793, 62
 Simon, J. D., et al. 2011, *ApJ*, 733, 46
 The Dark Energy Survey Collaboration. 2005, *ArXiv Astrophysics e-prints*
 Tollerud, E. J., Bullock, J. S., Strigari, L. E., & Willman, B. 2008, *ApJ*, 688, 277
 Tonry, J. L., et al. 2012, *ApJ*, 750, 99
 Tyson, J. A. 2002, in *Society of Photo-Optical Instrumentation Engineers (SPIE) Conference Series*, Vol. 4836, *Survey and Other Telescope Technologies and Discoveries*, ed. J. A. Tyson & S. Wolff, 10–20
 Vargas, L. C., Geha, M., Kirby, E. N., & Simon, J. D. 2013, *ArXiv e-prints*, *arXiv:1302.6594*
 Walsh, S. M., Willman, B., & Jerjen, H. 2009, *AJ*, 137, 450
 Walsh, S. M., Willman, B., Sand, D., Harris, J., Seth, A., Zaritsky, D., & Jerjen, H. 2007, *ArXiv e-prints*, *ApJ submitted*, *arXiv:0712.3054*, 712
 Willman, B., et al. 2005, *AJ*, 129, 2692
 Willman, B., Geha, M., Strader, J., Strigari, L. E., Simon, J. D., Kirby, E., Ho, N., & Warren, A. 2011, *AJ*, 142, 128
 Willman, B., & Strader, J. 2012, *AJ*, 144, 76
 York, D. G., et al. 2000, *AJ*, 120, 1579